ELSEVIER

Journal of Alloys and Compounds 356–357 (2003) 750–754

Journal of ALLOYS AND COMPOUNDS

www.elsevier.com/locate/jallcom

An electrochemical study of mono-substituted intermetallic hydrides

R. Baddour-Hadjean[a,*], H. Mathlouthi[d], J.P. Pereira-Ramos[b], J. Lamloumi[d], M. Latroche[c], A. Percheron-Guégan[c]

[a]*LADIR, CNRS UMR 7075, 2 rue Henri Dunant, 94320 Thiais, France*
[b]*LECSO, CNRS UMR 7582, 2 rue Henri Dunant, 94320 Thiais, France*
[c]*LCMTR, CNRS UPR 209, 2 rue Henri Dunant, 94320 Thiais, France*
[d]*L.M.M.P., ESSTT, 5 Avenue Taha Hussein, 1008 Tunis, Tunisie*

Received 5 September 2002; received in revised form 20 December 2002; accepted 1 February 2003

Abstract

The electrochemical behaviour of $LaNi_{2.5}Co_{2.5}$, $LaNi_{4.5}Mn_{0.5}$ and $LaNi_{4.5}Al_{0.5}$ intermetallic compounds was investigated using chronopotentiometric and impedance measurements. Electrochemical isotherms have been found to be in good agreement with solid gas determinations. Kinetics data are drawn from impedance spectroscopy for the three compounds. Important changes in the magnitude of a low frequency semicircle in the impedance diagrams have been correlated to a corrosion layer effect which is strongly reduced from the first cycle and as cycling proceeds. A subsequent increase in the apparent hydrogen chemical diffusion coefficient D_H is found from the first cycle, which is well correlated to the decrease of the diffusion length through the oxide layer as the thickness of the corrosion layer decreases. The apparent hydrogen chemical diffusion coefficient is found to be one order of magnitude larger in the α phase (10^{-10} cm^2/s) than in the β phase.

Keywords: Intermetallics; AB_5 hydrogen storage alloys; Ni–MH battery; Impedance spectroscopy; Hydrogen transport

1. Introduction

From the point view of the electrochemical storage application, $LaNi_5$ is the most promising negative electrode material for rechargeable Ni–MH batteries because of the rapid and reversible storage of large quantities of hydrogen [1]. However the practical application of $LaNi_5$ is limited both from a thermodynamic and an electrochemical point of view: the hydride formation pressure is too high (~ 1.7 bars) and the capacity loss of such an electrode upon cycling is too large for practical application (50% loss of capacity upon 100 cycles). It is nevertheless possible to overcome such limitations by changing the composition of the parent $LaNi_5$ alloy. Partial substitutions on the lanthanum and the nickel sites have been proved to be very successful in adapting the thermodynamic properties of the hydrides and improving their life time upon cycling and the best compromise has been found for the three substituted $LaNi_{3.55}Mn_{0.4}Al_{0.3}Co_{0.75}$ compound [2]. However, it remains that in spite of such effects of the composition on the long-term electrochemical behaviour, little is known about its origin and the specific effect of each substituent.

In this study, single substituted $LaNi_{4.5}Mn_{0.5}$, $LaNi_{4.5}Al_{0.5}$ and $LaNi_{2.5}Co_{2.5}$ compounds were systematically examined to get further detailed information concerning the impact of each Mn, Al and Co substituent on the negative electrode behaviour. The performance of the negative electrode is mainly controlled by the kinetics of the hydrogen diffusion process and/or the reactions taking place on the alloy surface. Electrochemical impedance spectroscopy is a powerful tool in such a context as it allows to get an understanding of the different processes if their time constants are well separated. However, till now very few data have been reported for the single substituted compounds. Most of the kinetic studies concern the conventional trisubstituted compounds [3–16] and only one paper reports an apparent chemical hydrogen diffusion coefficient for $LaNi_{4.5}Al_{0.5}$, determined by the potential step electrochemical technique [17]. Moreover, examination of the first charge–discharge cycles by electrochemical impedance spectroscopy (EIS) has only been reported by Yang et al. [16] for a Mm-based multicomponent alloy.

*Corresponding author.
E-mail address: rita.badour@glvt-cnrs.fr (R. Baddour-Hadjean).

0925-8388/03/$ – see front matter
doi:10.1016/S0925-8388(03)00351-7

In this paper, electrochemical features such as discharge capacity, potential composition isotherms and cycling behaviour are reported for each single substituted $LaNi_{4.5}Mn_{0.5}$, $LaNi_{4.5}Al_{0.5}$ and $LaNi_{2.5}Co_{2.5}$ compounds. Changes in the impedance spectra all over the first 10 cycles are discussed and values for the exchange current density and apparent hydrogen chemical diffusion coefficient are reported.

2. Experimental

All the intermetallic compounds were prepared as reported in Ref. [18]. The composite anodic electrodes were made from the intermetallic active powder (50 mg) with average particle size 40 μm mixed with carbon black and PTFE in the weight ratio of 90:5:5. The mixtures were spread out in sheets 0.25 mm thick and compressed up to 5 t on the two faces of a nickel grid ($S=0.65$ cm^2). Electrochemical measurements were conducted at room temperature in a conventional three-electrode cell. The electrolyte consisted of a 1 M KOH solution in which a continuous flow of Ar is kept through the cell. Impedance experiments were carried out after charging the electrode at 0.1 H/f.u. and waiting until the equilibrium potential is reached (~ 3 h). Kinetic measurements were performed in a frequency range from 10^5 Hz to 10^{-4} Hz using seven frequencies per decade, applying a computer-controlled 1255 Schlumberger frequency response analyser coupled to an EGG potentiostat model 273A. The excitation signal was 10 mV peak to peak.

3. Results and discussion

All the $LaNi_{5-x}M_x$ compounds crystallise in the original $P6/mmm$ $LaNi_5$ structure. However, an effect of partial Ni replacement is the increase of the unit cell volume in the order Ni<Co<Al<Mn (see Table 1). The expansion ratio of the corresponding cell volumes by solid gas hydrogen absorption at 25 °C is in the order Co<Al<Mn<Ni.

The hydriding properties of the single substituted $LaNi_{5-x}M_x$ (M=Al, Mn, Co) alloys are illustrated by the electrochemical potential–composition isotherm curves reported in Fig. 1. Such isotherms have been obtained from

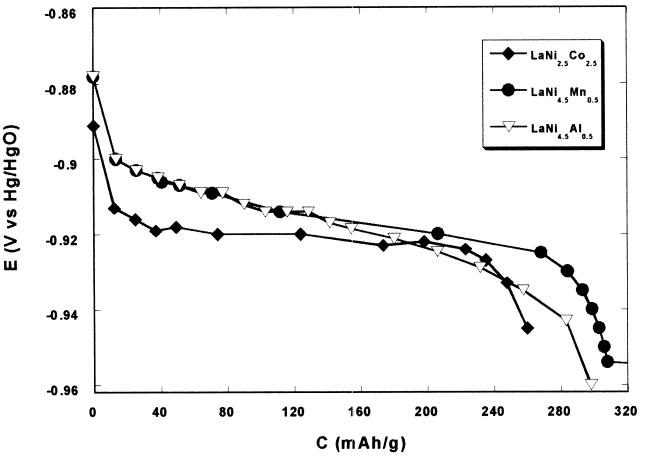

Fig. 1. Electrochemical discharge isotherms at 25 °C for $LaNi_{5-x}M_x$ intermetallic compounds.

OCV measurements during the charge process using the current pulse relaxation method except for the Mn-compound for which a dissolution process takes place. In that case, quasi equilibrium data have been achieved using galvanostatic charge curves at very low rate (5 mA/g). For the Co-compound, for which two equilibrium plateaus may exist and two related β and β′ hydrides [19], the present data are focused on the first plateau.

Table 2 reports the electrochemical and solid gas data for the different alloys, where the hydrogen absorption pressures P_{H2} have been converted into equilibrium electrode potential E_{eq}^{SG} using the Nernst equation [20].

In addition to the expected effect of Ni substitution on the hydride formation pressure, lower discharge capacities are available compared to the parent $LaNi_5$ compound, which range between 250 and 310 mAh/g. A good agreement is found between the solid gas and electrochemical data within the experimental error, both from the view-point of potentials and specific capacities. A probable dissolution process taking place for $LaNi_{4.5}Mn_{0.5}$ could explain the higher discrepancy between the two sets of data.

Results of cyclic galvanostatic experiments at $C/3$, $D/6$ rates are illustrated in Fig. 2 by the evolution of the discharge capacity vs. number of cycles. In spite of a very fast activation, $LaNi_{4.5}Mn_{0.5}$ exhibits a strong decline of the capacity during the first 20 cycles and stabilises thereafter around 200 mAh/g. For $LaNi_{4.5}Al_{0.5}$, a maxi-

Table 1
Cell parameters and volume of material electrodes

Compound	a(Å) ±0.005	c (Å) ±0.01	V (Å^3) ±0.04	$\Delta V/V$[a] (%)
$LaNi_5$	5.012	3.984	86.68	25.0
$LaNi_{2.5}Co_{2.5}$	5.054	3.988	88.19	14.6
$LaNi_{4.5}Al_{0.5}$	5.034	4.022	88.27	19.5
$LaNi_{4.5}Mn_{0.5}$	5.050	4.018	88.74	22.0

[a] The expansion ratio of cell volume by solid gas hydrogen absorption at 25 °C.

Table 2
Solid gas and electrochemical data for the different $LaNi_{5-x}M_x$ alloys

Compound	P_{H2} (bars)	E_{eq}^{SG} (mV)	E_{dis} (mV)	$C_{at\ 1\ bar,\ 25\ °C}$ (mAh/g)	C_{dis} (mAh/g)
$LaNi_{2.5}Co_{2.5}$	0.20	−917	−920	250	250
$LaNi_{4.5}Al_{0.5}$	0.16	−914	−915	300	280
$LaNi_{4.5}Mn_{0.5}$	0.11	−910	−915	380	310

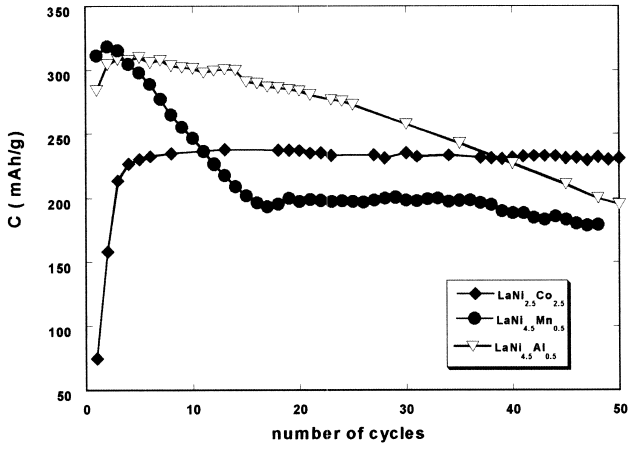

Fig. 2. Evolution of the specific capacity with the number of cycles for $LaNi_{5-x}M_x$ compounds (KOH 1 N, *C*/3, *D*/6 rates).

mum capacity of 310 mAh/g is rapidly available, which decreases continuously to reach 200 mAh/g after 50 cycles. Insofar as the expansion ratio of the unit cell volume is very close for both compounds (Table 1), the more severe decrease observed for the Mn-compound is probably associated to a noticeable dissolution process in alkaline electrolyte [21]. Conversely, the discharge capacity of the $LaNi_{2.5}Co_{2.5}$ needs about 10 cycles before reaching its maximum values of 240 mAh/g, very close to the theoretical one and remains stable at least over 50 cycles. The lower value of the volume expansion (Table 1) can explain the positive effect of cobalt on cycling stability as a consequence of a limited decrepitation process.

The kinetics of hydrogen transfer and hydrogen diffusion in the bulk alloys has been investigated using EIS. Typical impedance diagrams are reported in Fig. 3 for $LaNi_{2.5}Co_{2.5}$ for the same state of charge of 0.1 H/f.u. (~ 6 mAh/g) corresponding to the α phase solid solution, after a varying number of charge–discharge cycles during the first 10 cycles. All these spectra consist of a very small semicircle in the high frequency region (10^5 Hz–10^2 Hz), a slope of about 45° related to Warburg impedance in the medium frequency range (10^2 Hz–1 Hz), and a large semicircle in the low frequency region (1 Hz–10^{-4} Hz), which exhibits marked dependence on the cycle number: its contribution significantly decreases during the first cycles: from 330 Ω for the raw material to 40 Ω after one cycle and 8Ω after 10 cycles for $LaNi_{2.5}Co_{2.5}$ (Fig. 3a). A less pronounced trend is observed for $LaNi_{4.5}Al_{0.5}$ as the initial impedance of the low frequency semicircle is far lower: only 18 Ω for the raw material, 7 Ω after one cycle and 4Ω after 10 cycles.

Furthermore, long-time immersion of a cycled $LaNi_{2.5}Co_{2.5}$ electrode in KOH 1 N in open circuit condition gives evidence for an increase of the low frequency semicircle: the impedance associated changes from 5 to 18 Ω after 2 days of storage, and the corresponding capacitance decreases by a factor 3. This phenomenon indicates that the low frequency response corresponds to the presence of a corrosion layer whose thickness increases with time immersion. Therefore, the very high impedance of 330 Ω observed for the raw $LaNi_{2.5}Co_{2.5}$ material reflects the presence on the alloy surface of a great amount of native oxides and/or corrosion products formed in the KOH electrolyte [21].

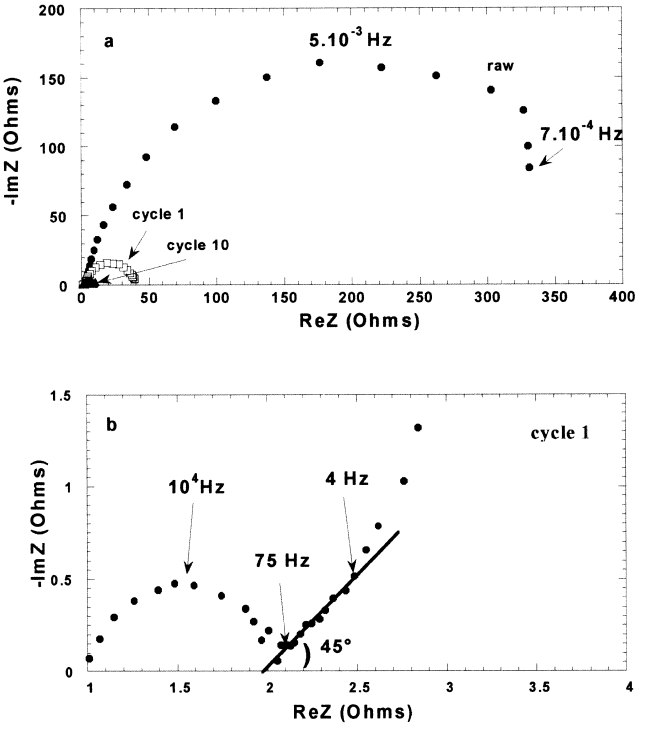

Fig. 3. (a) Typical Nyquist plots for $LaNi_{2.5}Co_{2.5}H_{0.1}$ during the first 10 cycles. (b) Enlarged view of the Warburg region for $LaNi_{2.5}Co_{2.5}H_{0.1}$ (first cycle).

Conversely, whatever the intermetallic compound, the high frequency semicircle with a characteristic frequency of 10^4 Hz remains practically unchanged with cycle number, state of charge or time exposure in KOH. The value of the resistance associated with this fastest step remains stable all over the first cycles for the three compounds. (R~1/1.5 Ω for $LaNi_{2.5}Co_{2.5}$ and $LaNi_{4.5}Mn_{0.5}$, R~5 Ω for $LaNi_{4.5}Al_{0.5}$). The assignment of this small arc is not very clear at the moment and is still a matter of controversy. It was first attributed to the contact resistance between the hydrogen storage alloy and the current collector and between the alloys particles [22,23]. However more recently, based on impedance modelling of the kinetics of metal hydride electrodes, Wang [24] attributed the features at high frequency to the charge transfer reaction. Experimentally, such a high frequency small arc was also observed for hydrogen storage alloy ingot [12], which makes questionable its assignment to a contact resistance. Furthermore, from our results we can find that the capacitance value for the high frequency region (C~ 15–20 μF/cm^2) is consistent with the double layer

capacitance expected at the metal-solution interface [25]. This value is almost constant whatever the cycle number. Hence, the high frequency semicircle can be mainly regarded as the charge transfer process, as previously reported [16,24]. Exchange current density values J_0 of 20 and 4 mA/cm^2, respectively, for $LaNi_{2.5}Co_{2.5}$ and $LaNi_{4.5}Al_{0.5}$ are then obtained from the charge transfer resistance. Such values are in good agreement with those reported in the literature for intermetallic compounds [16,26].

Fig. 3b allows to clearly distinguish at medium frequencies (4 to 75 Hz) a straight line with an angle of 45° corresponding to the 'Warburg region'. In this frequency range, under semi-infinite diffusion conditions, the apparent chemical diffusion coefficient of hydrogen D_H can be calculated from the Warburg's prefactor A (slope of the plots ReZ vs. $\omega^{-1/2}$)

$$A\,(\Omega.s^{-1/2}) = [Vm\,(dE/dx)]/[(2D_H)^{1/2}.F.S]$$

where V_m is the molar volume (53 cm^3), dE/dx is the slope of the coulometric titration curve for a given x value, determined from Fig. 1 and S is the geometric area (1.3 cm^2).

Fig. 4 shows the slopes of the plots ReZ vs. $\omega^{-1/2}$ for $LaNi_{2.5}Co_{2.5}H_{0.1}$ as a function of the cycle number. The Warburg's prefactor A is found to decrease from 5.7 $\Omega.s^{-1/2}$ for the raw material to 1.1 $\Omega.s^{-1/2}$ for cycle 10. An apparent chemical diffusion coefficient of hydrogen D_H in $LaNi_{2.5}Co_{2.5}$ is found to increase from $4\cdot10^{-11}$ cm^2/s for the raw material to $2\cdot10^{-10}$ cm^2/s for the first cycle and 10^{-9} cm^2/s after 10 cycles. This increase is well correlated to the progressive decrease of the polarisation in charge–discharge curves during the first 10 cycles (from 270 to 70 mV) and the simultaneous increase in the specific capacity (from 70 to 240 mAh/g, see Fig. 2). The change in D_H by one order of magnitude, occurring between the raw material and the first cycle, cannot be explained by an increase in surface area usually described as a consequence of the decrepitation process. Indeed, the low capacity involved during the first discharge (70 mAh/g) cannot lead to a significant volume change in the electrode material. However the apparent hydrogen diffusion coefficient takes into account two factors: hydrogen transport in the bulk material and diffusion through a corrosion layer. Hence, the existence of native oxides and corrosion products at the electrode surface of the raw material can explain: (i) the high initial electrode impedance value (330 Ω); (ii) the correlated high polarisation in the first charge–discharge curves; and (iii) the lower initial D_H value. With a partial consumption of these oxides during the first reduction process, an increase of the rate of hydrogen transport is then observed.

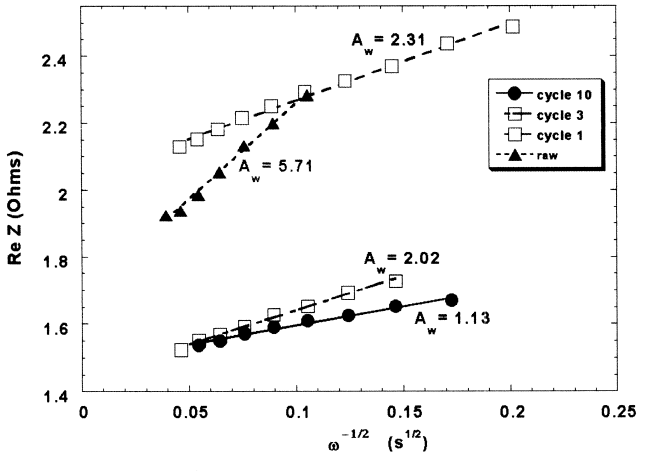

Fig. 4. ReZ vs. $\omega^{-1/2}$ plots for $LaNi_{2.5}Co_{2.5}H_{0.1}$ during the first 10 cycles.

In the case of the Al-based compound, an apparent chemical diffusion coefficient of hydrogen D_H is found to increase from $1.5\cdot10^{-11}$ cm^2/s for the raw material to $4\cdot10^{-11}$ cm^2/s for the first cycle and 10^{-10} cm^2/s after 10 cycles. These values are in good accordance with those determined by other techniques [27,28].

In contrast to the Co-compound, a very low increase in D_H is observed between the raw Al-based material and the first cycle. The value of the initial electrode impedance is twenty times lower compared to that of the Co-compound, and as a consequence, a good efficiency of the charge discharge process is observed from the first cycle (see Fig. 2).

Such different behaviours between the two compounds can mainly be explained by the nature and/or amount of the corrosion products. Indeed, cobalt-containing alloys are known to produce insoluble corrosion products such as Co, $Co(OH)_2$ and CoOOH at the alloy surface while no corrosion products related to Al is formed in the case of Al-based compounds [21]. This effect is especially enhanced in $LaNi_{2.5}Co_{2.5}$ characterised by a high cobalt content. These features explain the increase in the electrode impedance and the decrease in the apparent hydrogen diffusion coefficient which are commonly reported as the cobalt content is increased in multicomponent alloys [10,29] or as cobalt powder is added to metal hydride electrodes [12].

For both compounds, the apparent chemical diffusion coefficient is found to increase by half a decade between the first and the tenth cycle. A continuous decrease in the corrosion layer thickness on cycling could explain this result. Indeed, the value of the corrosion layer capacitance calculated from the characteristic frequency of the low frequency semicircle continuously increases with cycling: by 50% from the raw material to the first cycle, then once again by 40% between cycle 1 and cycle 10.

Similar EIS experiments performed on the Mn-Compound (Fig. 5) reveal a faster hydrogen diffusion in the α phase compared to the β phase by one order of magnitude: 10^{-10} to 10^{-11} cm^2/s, respectively. The parameters of the EIS response do not practically change with the state of

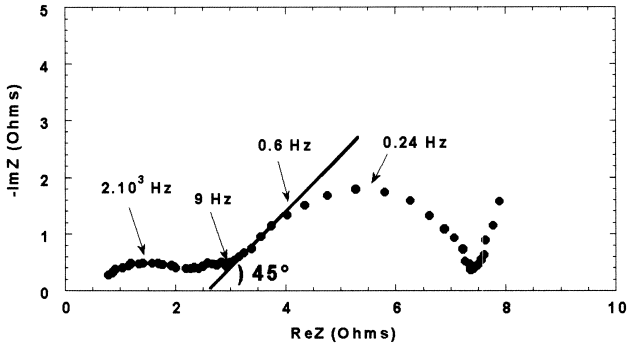

Fig. 5. Typical Nyquist plot for $LaNi_{4.5}Mn_{0.5}H_4$ at the 20th cycle.

charge and the number of cycles up to the 20th cycle, which could indicate that the key factor for the capacity drop for the Mn compound is not related to intrinsic kinetic limitations but to a rapid dissolution process.

4. Conclusion

This study of $LaNi_{5-x}M_x$ (M = Co, Al, Mn) compounds shows the surface properties of these materials govern their electrochemical behaviour. Galvanostatic and impedance measurements suggest the presence of a native corrosion layer in $LaNi_{2.5}Co_{2.5}$. This layer is responsible for the high initial electrode impedance. During the very first charge–discharge cycles, the layer thickness decreases as a consequence of the partial reduction of the native oxides and corrosion products: the resistance associated with the oxide layer decreases and its capacitance increases. This effect leads to an improvement of the hydrogen kinetics, as illustrated by the large increase in the apparent hydrogen diffusion coefficient, and better electrochemical efficiencies, as illustrated by the increasing capacities. Conversely, moderate effects take place for $LaNi_{4.5}Al_{0.5}$ and $LaNi_{4.5}Mn_{0.5}$ compounds for which a very fast activation process is observed. For all compounds, a further increase in the apparent hydrogen diffusion coefficient by half a decade is found between the first and tenth cycle. Additional experiments are needed to get a better insight into: (i) the mechanism occurring at the different time constants and (ii) the chemical and kinetic parameters governing the long-term cycling behaviour of each intermetallic's composition.

References

[1] A. Percheron-Guégan, J.C. Achard, J. Sarradin, G. Bronoël, Electrode material based on lanthanum and nickel, electrochemical uses of such materials, French Patents 75 16160, (1975); 77 23812, (1977); US patent 688537, (1978).
[2] H. Ogawa, M. Ikoma, H. Kawano, I. Matsumoto, J. Power Sources 12 (1988) 393.
[3] L.O. Valoen, S. Sunde, R. Tunold, J. Alloys Comp. 253–254 (1997) 656.
[4] L.O. Valoen, A. Lasia, J.O. Jensen, R. Tunold, Electrochim. Acta 47 (2002) 2871.
[5] A. Lundqvist, G. Lindbergh, J. Electrochem. Soc. 145 (11) (1998) 3740.
[6] H. Senoh, K. Morimoto, H. Inoue, C. Iwakura, P.H.L. Notten, J. Electrochem. Soc 147 (7) (2000) 2451.
[7] X. Yuan, N. Xu, J. Alloys Comp. 316 (2001) 113.
[8] X. Yuan, N. Xu, J. Alloys Comp. 329 (2001) 115.
[9] C. Weixiang, J. Power Sources 90 (2000) 201.
[10] C. Iwakura, K. Fukuda, H. Senoh, H. Inoue, M. Matsuoka, Y. Yamamoto, Electrochim. Acta 43 (14–15) (1998) 2041.
[11] W. Zhang, A. Visintin, S. Srinivasan, A.J. Appleby, H.S. Lim, J. Power Sources 75 (1998) 84.
[12] A. Yuan, N. Xu, J. Alloys Comp. 322 (2001) 269.
[13] H. Pan, Y. Chen, C. Wang, J.X. Ma, C.P. Chen, Q.D. Wang, Electrochim. Acta 44 (1999) 2263.
[14] H.S. Kim, M. Nishizawa, I. Uchida, Electrochim. Acta 45 (1999) 483.
[15] J. Chen, S.X. Dou, D.H. Bradhurst, H.K. Liu, Int. J. Hydrogen Energy 23 (3) (1998) 177.
[16] H. Yang, Y. Zhang, Z. Zhou, J. Wei, G. Wang, D. Song, X. Cao, C. Wang, J. Alloys Comp. 231 (1995) 625.
[17] T. Nishina, H. Ura, I. Uchida, J. Electrochem. Soc. 144 (4) (1997) 1273.
[18] R. Baddour-Hadjean, L. Meyer, J.P. Pereira-Ramos, M. Latroche, A. Percheron-Guégan, Electrochimica Acta 46 (2001) 2385.
[19] H.H. Van Mal, K.H.J. Buschow, A. Kuijpers, J. Less-Common Met. 32 (1973) 289.
[20] C. Iwakura, T. Asaoka, H. Yoneyama, T. Sakai, K. Oguro, H. Ishikawa, Nippon Kagaku Kaishi 1482 (1988).
[21] F. Maurel, B. Knosp, M. Backhaus-Ricoult, J. Electrochem. Soc. 147 (1) (2000) 78.
[22] N. Kuriyama, T. Sakai, H. Miyamura, I. Uehara, H. Ishikawa, J. Alloys Comp. 202 (1993) 183.
[23] W. Zhang, M.P. Kumar, S. Srinivasan, H.J. Ploehn, J. Electrochem. Soc. 142 (9) (1995) 2935.
[24] C. Wang, J. Electrochem. Soc. 145 (6) (1998) 1801.
[25] J. Bard, R. Faulkner, Electrochimie: Principes, Méthodes et Applications, Masson, Paris, New York, 1983.
[26] B.V. Ratnakumar, C. Witham, B. Fultz, G. Halpert, J. Electrochem. Soc. 141 (8) (1994) L89.
[27] G. Zheng, B.N. Popov, R.E. White, J. Electrochem. Soc. 142 (1995) 2695.
[28] M. Geng, J. Han, F. Feng, D.O. Northwood, J. Electrochem. Soc. 146 (1999) 3591.
[29] H. Pan, J. Ma, C. Wang, C.P. Chen, Q.D. Wang, Electrochim. Acta 44 (1999) 3977.